Supplemental Figure 1

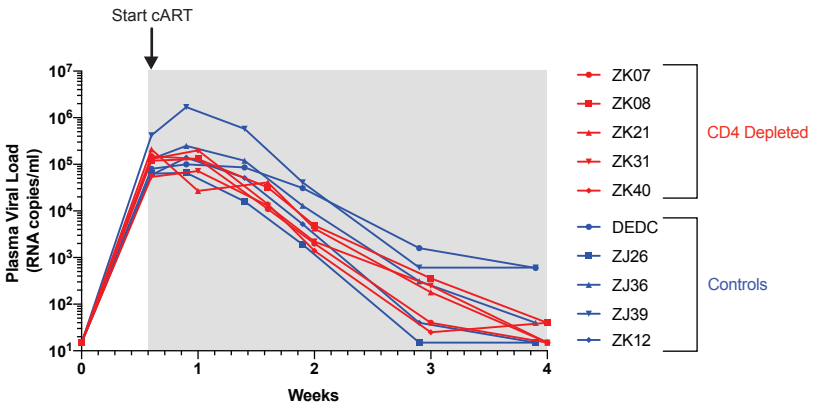

Supplemental Figure 1. Plasma viral loads through 4 weeks of SIV infection. SIV RNA was quantified in longitudinal plasma samples using a qRT-PCR assay with a threshold quantification limit of 15 vRNA copies/ml. Shown are the values for the first 4 weeks of the study, which include pre-cART time points and the first 24 days on cART (gray shaded region). CD4-depletion experimental group animals are shown with red plots; control animals are shown with blue plots.

Supplemental Figure 2

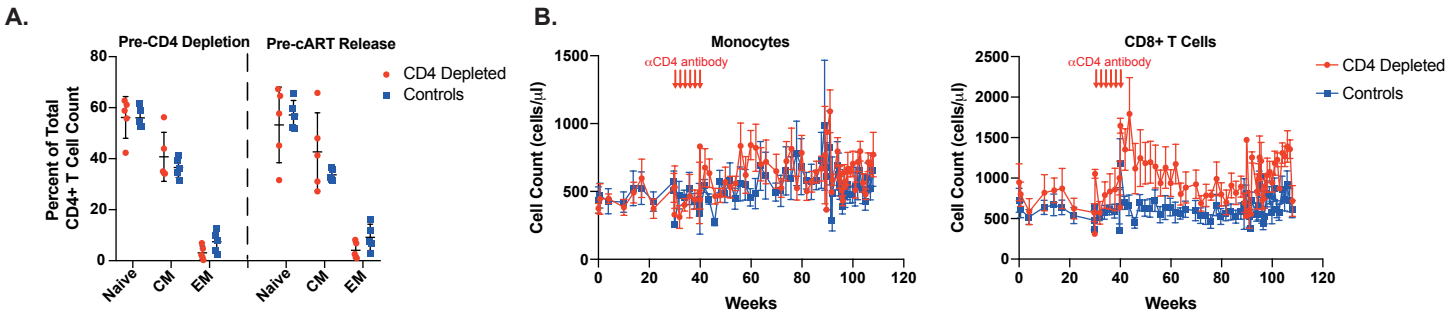

Supplemental Figure 2. Cell population changes with CD4 depletion. A) The frequency of naïve (CD95-), central memory (CD95+ CD28+), and effector memory (CD95+ CD28-) CD4+ T cells in blood prior to CD4 depletion and prior to cART release (one year after the final dose of anti-CD4 antibody) are shown for CD4 depleted (red) and control (blue) group animals. Lines and bars represent medians and interquartile ranges. B) Longitudinal mean +/- the standard error of the means monocyte (left) and CD8+ T cell counts (right) in blood of CD4 depleted (red, n=5) and control (blue, n=5) group animals prior to and after anti-CD4 antibody administrations (red arrows).

Supplemental Figure 3

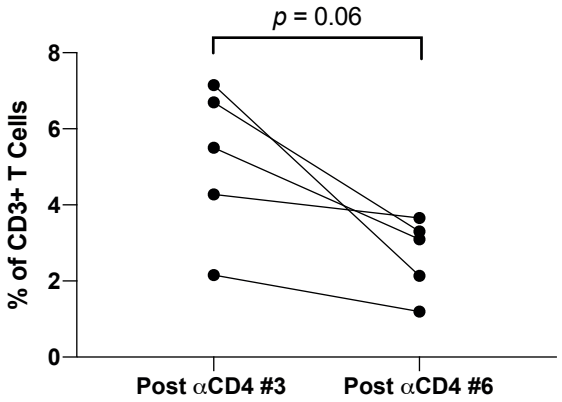

Supplemental Figure 3. Change in central memory CD4+ T cells in LN tissues with additional anti-CD4 antibody administrations. Shown is a comparison of frequencies of central memory (CD95+ CD28+) CD4+ T cells following 3 or 6 doses of anti-CD4 antibody for each of the 5 CD4 depleted study animals. Data were statistically analyzed using a one-tailed Wilcoxon rank-sum test.

Supplemental Figure 4

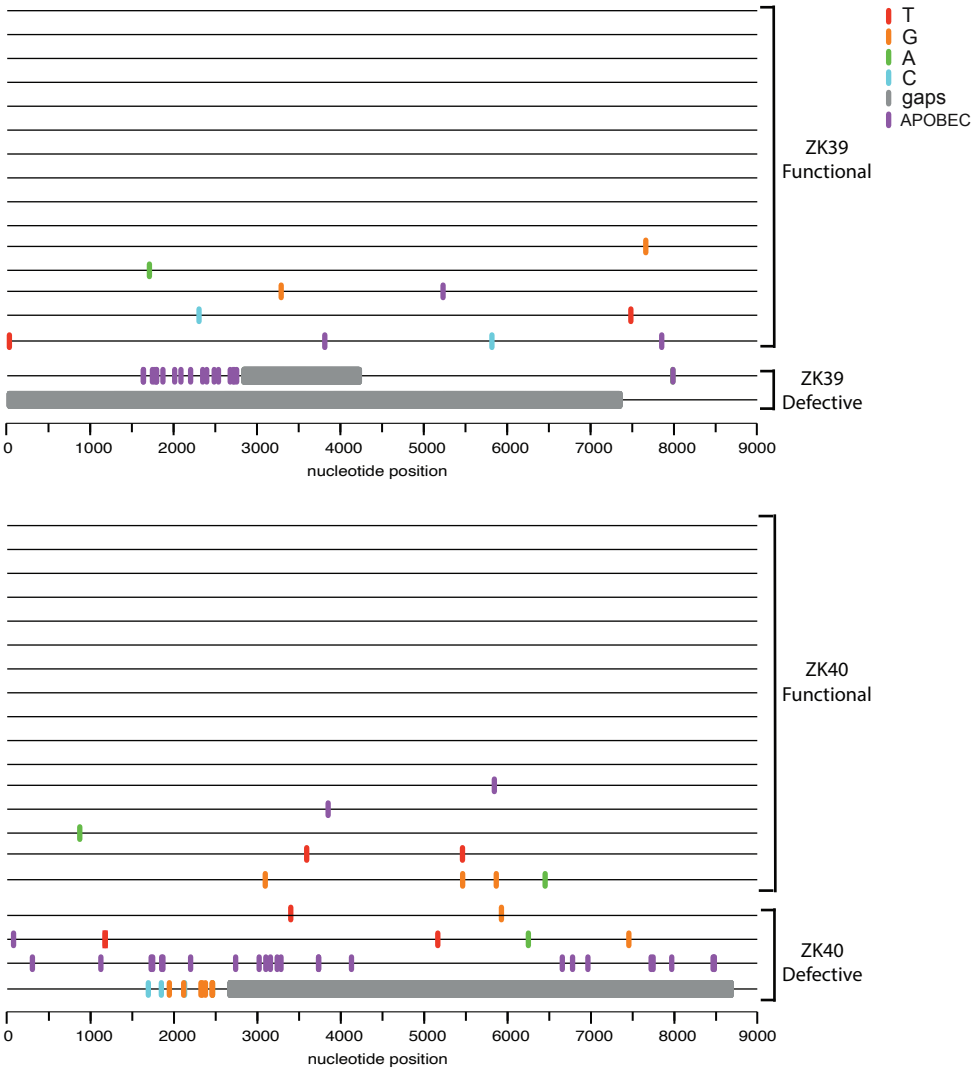

Supplemental Figure 4. Near full-length viral DNA genome sequencing. Near full-length viral genome sequencing was performed on viral DNA extracted from lymph node-derived mononuclear cells collected from the indicated animals immediately prior to the first anti-CD4 antibody administration. Individual nucleotide polymorphisms relative to the parental SIVmac239 sequence are indicated by colored ticks in the shown highlighter plots. Sequences containing premature stop codons, extensive hypermutations, or deletions were scored as “non-functional”, while other sequences were scored as “functional”.

Supplemental Figure 5

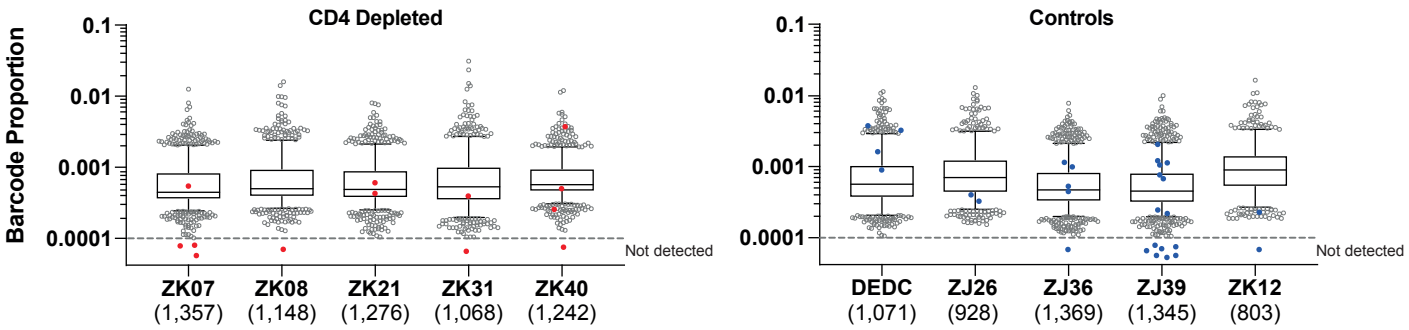

Supplemental Figure 5. SIVmac239M viral clonotypes distribution prior to cART. Deep sequencing analysis was performed on the barcode insert region of the SIVmac239M RNA genomes in plasma at peak viral load prior to cART for each study animal. The distributions of the relative clonotype proportions are shown. For each animal, the box delineates the interquartile range and the whiskers delineate the 5th and 95th percentile of the distribution. The number in parentheses below each animal is the number of clonotypes detected. Colored circles show the location within the pre-cART distribution for clonotypes that rebounded upon cART cessation. Rebound clonotypes that were not detected in plasma prior to cART initiation are shown below the dashed line.

Supplemental Figure 6

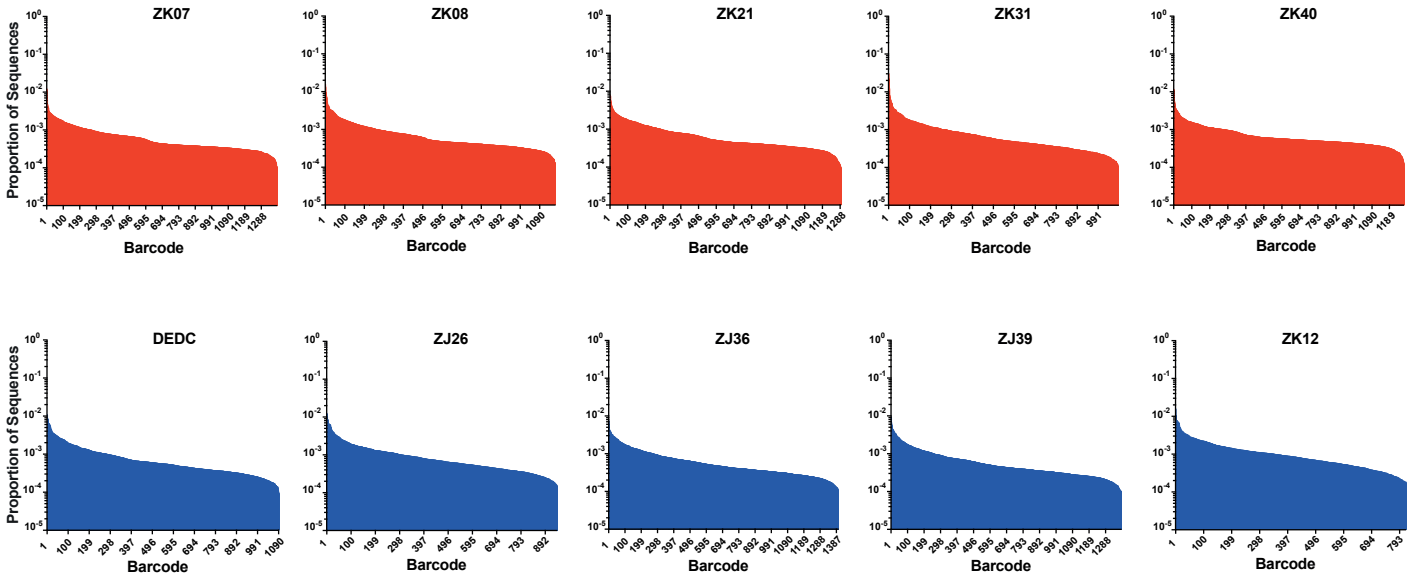

Supplemental Figure 6. SIVmac239M viral clonotype proportions prior to cART. Shown are bar graphs depicting the relative proportion of the total virus population for each viral clonotype identified in each study animal prior to cART initiation. Data for CD4-depleted animals are shown in red; control animals are shown in blue.

Supplemental Figure 7

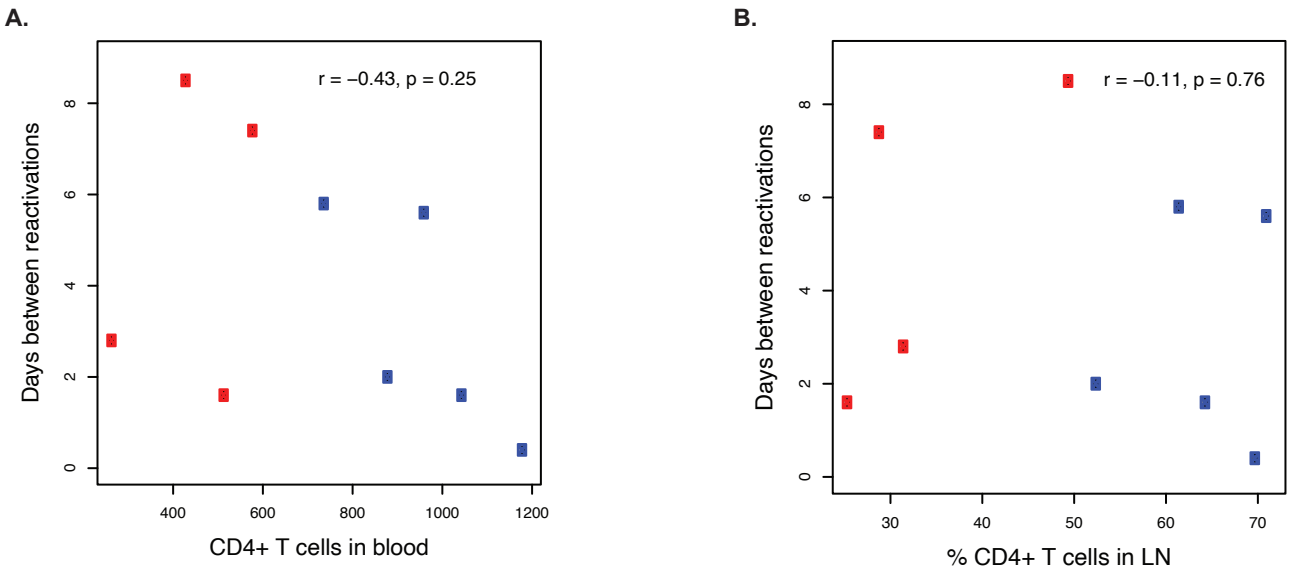

Supplemental Figure 7. Correlation between CD4 level and viral reactivation rate. The relationships between CD4+ T cell count in blood (A) and % CD4+ T cells in LN tissue (B) at the time of cART discontinuation vs the calculated reactivation rate for CD4-depleted (red) and control group (blue) animals are shown. The data were analyzed using the Pearson correlation coefficient.